

THE OFFICIAL MAGAZINE OF THE OCEANOGRAPHY SOCIETY

Oceanography

CITATION

Fiedler, J.W., M.A. McManus, M.S. Tomlinson, E.H. De Carlo, G.R. Pawlak, G.F. Steward, O.D. Nigro, R.E. Timmerman, P.S. Drupp, and C.E. Ostrander. 2014. Real-time observations of the February 2010 Chile and March 2011 Japan tsunamis recorded in Honolulu by the Pacific Islands Ocean Observing System. *Oceanography* 27(2):186–200, <http://dx.doi.org/10.5670/oceanog.2014.34>.

DOI

<http://dx.doi.org/10.5670/oceanog.2014.36>

COPYRIGHT

This article has been published in *Oceanography*, Volume 27, Number 2, a quarterly journal of The Oceanography Society. Copyright 2014 by The Oceanography Society. All rights reserved.

USAGE

Permission is granted to copy this article for use in teaching and research. Republication, systematic reproduction, or collective redistribution of any portion of this article by photocopy machine, reposting, or other means is permitted only with the approval of The Oceanography Society. Send all correspondence to: info@tos.org or The Oceanography Society, PO Box 1931, Rockville, MD 20849-1931, USA.

Real-Time Observations of the February 2010 Chile and March 2011 Japan Tsunamis Recorded in Honolulu by the Pacific Islands Ocean Observing System

BY JULIA W. FIEDLER, MARGARET A. McMANUS, MICHAEL S. TOMLINSON,
ERIC H. DE CARLO, GENO R. PAWLAK, GRIEG F. STEWARD, OLIVIA D. NIGRO,
ROSS E. TIMMERMAN, PATRICK S. DRUPP, AND CHRIS E. OSTRANDER



Sediment plume issuing from the Ala Wai Boat Harbor and entering Māmala Bay at Waikiki. This photo was taken at 1457 HST on March 11, 2011, about 11.5 hours after the arrival of the first tsunami wave at the Honolulu tide gauge and five hours after the end of the tsunami advisory. The boats are returning to the harbor following the evacuation. *Photo credit: Ross Timmerman*

ABSTRACT. Continuous monitoring by the Pacific Islands Ocean Observing System (PacIOOS) provided a unique opportunity to study the effects of two tsunamis on the coastal and estuarine waters of Hawai'i. By the time the 2010 Chile and 2011 Japan tsunamis reached the waters of southern O'ahu, they had lost much of their power (both were < 1 m high in Honolulu Harbor). Nevertheless, their effects on the surrounding waters were profound, with increases observed in near-bed current velocities, mixing in estuarine waters, salinity, turbidity, chlorophyll, and pathogenic bacteria such as *Vibrio* spp. In addition to these increases, we observed small decreases in nitrate and dissolved oxygen concentrations offshore, including a dampening of the normal diel cycle in dissolved oxygen. Some of the effects penetrated canals as far as 1 km inshore and could be observed up to 0.5 km offshore. Data from the PacIOOS sensors and our sampling show that altered and potentially degraded water quality can persist longer than the physical threat from surge. Shortly after both tsunamis, the "all clear" signal was given and people resumed recreational activities in coastal waters before our data indicated recovery of healthy water quality conditions. Following such events, monitoring should be expanded and continued in order to accurately characterize water quality and evaluate potential public health risks.

INTRODUCTION

On February 27, 2010, at 0634 UTC, a magnitude 8.8 earthquake struck the offshore Maule region of central Chile, with an epicenter at 35.909°S, 72.733°W, and a depth of 35 km. The earthquake triggered a trans-Pacific tsunami, with the first wave predicted to arrive at the Honolulu tide gauge at 1152 Hawaiian Standard Time (HST), Saturday, February 27 (Pacific Tsunami Warning Center/NOAA/NWS, 2010). Along the Chilean coastline, the tsunami produced waves ranging from 0.28 m at Iquique to as high as 11.2 m at Constitución. Most wave heights around the rest of the Pacific were less than 1 m. The tsunami reached the Honolulu tide gauge in 15.3 hours, shortly before 1200 HST with a maximum wave height of 0.98 m at Kahului, Maui, and 0.25 m at the Honolulu, O'ahu, tide gauge (National Geophysical Data Center, 2011a).

A little more than a year later, on

March 11, 2011, 0546 UTC, a magnitude 9.0 earthquake near Honshu, Japan (38.322°N, 142.369°E), with a depth of 32 km, generated another trans-Pacific tsunami. This tsunami caused catastrophic devastation and loss of life in Japan, and propagated damaging waves throughout the Pacific (National Geophysical Data Center, 2011b). The highest reported run-up, or difference between elevation of inundation line and sea level at the time of the tsunami, was 39.7 m at Miyako, Japan (Mori et al., 2011).

The tsunami reached Hawai'i in about 7.6 hours, with the maximum water height at the Honolulu tide gauge arriving slightly before the predicted arrival time of 0321 HST, March 11, 2011. The tsunami waves caused damage to infrastructure and personal property statewide. The Honolulu tide gauge reached a peak water height of 0.71 m at 0314 HST, whereas the Kahului,

Maui, tide gauge recorded a maximum water height of 2.00 m at 0327 HST. There are also eyewitness reports of water heights up to "11 to 12 ft" (3.35 to 3.66 m) at Nāpōpōpō on Hawai'i Island (Star-Advertiser Staff, 2011).

The Chile and Japan tsunamis, occurring roughly a year apart, provided a unique opportunity to compare their effects in Māmala Bay, O'ahu, Hawai'i, and in its tributaries under similar weather conditions. Here, we present water quality and physical oceanographic observations following the two tsunamis at Honolulu, as recorded by various components of the Pacific Islands Ocean Observing System (PacIOOS).

Much of the discussion of water quality impacts in scientific literature is limited to soil and/or groundwater quality resulting from tsunami inundation (Elango et al., 2006; Chandrasekharan et al., 2008; Newton and Icelly, 2008; Mattsson et al., 2009; Violette et al., 2009) and the debris introduced to surface waters (Tanabe and Subramanian, 2011). There are, however, also some data available on the impacts to surface water quality resulting from tsunamis (Reddy et al., 2005; Laluraj et al., 2007; Dharanirajan et al., 2007; Sarangi, 2011).

Reddy et al. (2005) sampled water quality along the Dakshina Kannada Coast (Southwest India) at their regular coastal water-monitoring program stations in January 2005 following the December 26, 2004, Indian Ocean tsunami. These data were compared with data collected from these same stations in January 2003 and 2004. Reddy et al. (2005) reported marginally higher pH values, a "drastic" reduction in dissolved oxygen (as low as 1.99 mg L⁻¹), salinity

elevated by about one salinity unit, and elevated concentrations of the nutrients phosphate (fourfold increase) and nitrate (twofold increase on average), but not silicate, following the Indian Ocean tsunami.

Laluraj et al. (2007) examined surface water quality effects in the Cochin estuary on the southwest coast of India four days after the arrival of the initial waves of the 2004 Indian Ocean tsunami and compared these data with conditions prior to and following this large tsunami. They reported a nearly 2°C drop in water temperature, the erosion of the seaward-extending salinity gradient with the high-salinity water from the tsunami, and a tenfold decrease in water transparency (Secchi depth) from values as high as 3.0 m prior to the tsunami to 0.3 m during the tsunami. They attributed the increased turbidity to the “churning up of the sea bed.” Like Reddy et al. (2005), Laluraj et al. (2007) reported a marginal increase in pH, but they reported only marginal changes in dissolved oxygen. Also, like Reddy et al. (2005), Laluraj et al. (2007) reported nitrate and phosphate concentrations that were two to three times higher during the tsunami,

which they attributed to sediment resuspension, but unlike Reddy et al. (2005), Laluraj et al. (2007) reported elevated concentrations of silicate and of ammonia, the latter as high as 93.3 μM.

Dharanirajan et al. (2007) mentioned water quality effects, but most of their discussion centered around tsunami debris, saltwater inundation of the land, and the effects of increased siltation on corals. They did state that “changes in water quality ha[ve] affected the biodiversity.”

Using satellite imagery obtained before, during, and after the 2004 Indian Ocean tsunami, Sarangi (2011) noted increased chlorophyll concentrations and decreased sea surface temperatures (SST) in portions of the Bay of Bengal during and following the tsunami. In the same article, Sarangi, using 2011 Moderate Resolution Imaging Spectroradiometer (MODIS) Aqua chlorophyll and SST data sets, noted high chlorophyll concentrations (2.0–2.5 mg m⁻³, presumably in the Pacific Ocean) after the tsunami struck Japan, but no significant change in SST.

Our PacIOOS observations allowed us to characterize the surface water quality and physical oceanographic effects

of relatively small tsunamis (locally). Our results showed that even a small amplitude tsunami can have profound water quality effects in semi-enclosed embayments, as well as discernible effects on the coastal environment.

METHODS

PacIOOS is committed to providing timely data essential to the health and safety of coastal waters. Components of PacIOOS used for this study include nearshore water quality sensors, water quality buoys, and the Kilo Nalu Observatory, which are all located on the south shore of O‘ahu in Māmalā Bay (Figure 1). In addition, water level and meteorological data were obtained from the National Oceanic and Atmospheric Administration (NOAA) National Ocean Service (NOS) Honolulu tide gauge (#1612340), as well as the US Geological Survey (USGS) Mānoa-Pālolo Drainage Canal (MPDC) stream gauge (#16274100) at Mō‘ili‘ili on the island of O‘ahu.

Nearshore Sensors

In 2010 and 2011, PacIOOS maintained four nearshore sensors on the south shore of O‘ahu (Figure 1). The first two, NS01 and NS02, were situated near the mouth of the Ala Wai Canal, at the Waikīkī and Hawai‘i Yacht Clubs, respectively. Nearshore sensors NS01 and NS02 consisted of SBE16plus V2 SEACAT® Sea-Bird Electronics sensors with attached WET Labs combination fluorescence and turbidity sensors (ECO FLNTUS®). NS01 and NS02 record temperature, conductivity, fluorescence (from which chlorophyll-*a* is estimated), and optical backscatter (as an approximation of turbidity). In February 2011, NS01 was redeployed to also record pressure. During the 2010

Julia W. Fiedler is a graduate student at Scripps Institution of Oceanography, University of California, San Diego, La Jolla, CA, USA. **Margaret A. McManus** is Professor, Department of Oceanography, University of Hawai‘i at Mānoa, Honolulu, HI, USA. **Michael S. Tomlinson** (mtomlins@hawaii.edu) is Staff Oceanographer, Department of Oceanography, University of Hawai‘i at Mānoa, Honolulu, HI, USA. **Eric H. De Carlo** is Professor, Department of Oceanography, University of Hawai‘i at Mānoa, Honolulu, HI, USA. **Geno R. Pawlak** is Associate Professor, Mechanical and Aerospace Engineering, University of California, San Diego, La Jolla, CA, USA. **Grieg F. Steward** is Associate Professor, Department of Oceanography, University of Hawai‘i at Mānoa, Honolulu, HI, USA. **Olivia D. Nigro** is Postdoctoral Researcher, Department of Oceanography, University of Hawai‘i at Mānoa, Honolulu, HI, USA. **Ross E. Timmerman** is a graduate student in the Department of Environmental Sciences, University of Virginia, Charlottesville, VA, USA. **Patrick S. Drupp** is a graduate student in the Department of Oceanography, University of Hawai‘i at Mānoa, Honolulu, HI, USA. **Chris E. Ostrander** is Assistant Dean, Department of Oceanography, University of Hawai‘i at Mānoa, Honolulu, HI, USA.

tsunami, both NS01 and NS02 recorded temperature and salinity ~ 0.15 m below the surface. NS02 turbidity (NTU) and fluorescence are also near-surface readings, while NS01, undergoing a float test at the time, recorded turbidity and fluorescence at a fixed depth (~ 0.70 m from bottom). During the 2011 tsunami, all NS01 measurements were made near the surface. NS03, located at the Hilton Pier in Waikīkī, and NS04, located just off the Waikīkī Aquarium, consist of SBE 37-SMP MicroCAT[®] Sea-Bird Electronics sensors. NS03 and NS04 record temperature, salinity, and pressure at depths of 0.94 m and 0.35 m from the bottom, respectively.

Pressure data from the nearshore sensors were high-pass filtered at a cut-off frequency of four cycles per day (cpd) to remove the regular tidal signal. Power spectra, using Welch's method, were then computed for each instrument to obtain estimates of wave period and power.

Water Quality Buoys

This study uses data from two PacIOOS/PMEL (NOAA's Pacific Marine Environmental Laboratory) MAPCO₂ water quality buoys located about 250–400 m offshore in ~ 12 m of water. The PMEL-designed MAPCO₂ buoys collect CO₂ data from surface seawater and marine boundary air every three hours; PacIOOS installed additional water quality sensors on these buoys and maintains the buoys for PMEL. Water quality buoy WQB-AW is located near the mouth of the Ala Wai Canal; WQB-KN is located near the Kilo Nalu Observatory (KNO; Figure 1). Each buoy is equipped with a Sea-Bird Electronics SBE16plus V2 SEACAT[®], SBE 43[®] dissolved oxygen membrane-type sensor, and a WET Labs ECO FLNTUS[®] combination fluorescence and turbidity

sensor. Both buoys measure temperature, conductivity, dissolved oxygen, fluorescence, optical backscatter (turbidity), and CO₂. In addition, late in 2010, after the Chile tsunami, WQB-AW was also equipped with a Satlantic ISUS V3[®] nitrate sensor. Unfortunately, WQB-KN was not operational at the time of the 2011 Japan tsunami due to routine annual maintenance.

Kilo Nalu Observatory

KNO consisted of a set of instruments cabled to shore power and extending from water depths of 12 m to 20 m offshore of Kaka'ako Waterfront Park in Honolulu (Figure 1). Baseline data included current magnitude and direction, pressure, and acoustic

intensity measured using a 1,200-kHz RD Instruments acoustic Doppler current profiler (ADCP). During the 2011 Japan tsunami, KNO observations were not available in real time due to technical issues; however, autonomous observatory instrumentation captured the tsunami signal.

Water Sampling and Quantitative Polymerase Chain Reaction Assay for *Vibrio* Abundance

Water samples (1 L) were collected as part of a year-long study in 2008 and 2009 (Nigro, 2012) and immediately following the 2011 Japan tsunami (only) from approximately 0.1–0.2 m depth in acid-washed, amber polyethylene bottles using a swing sampler (Nasco)

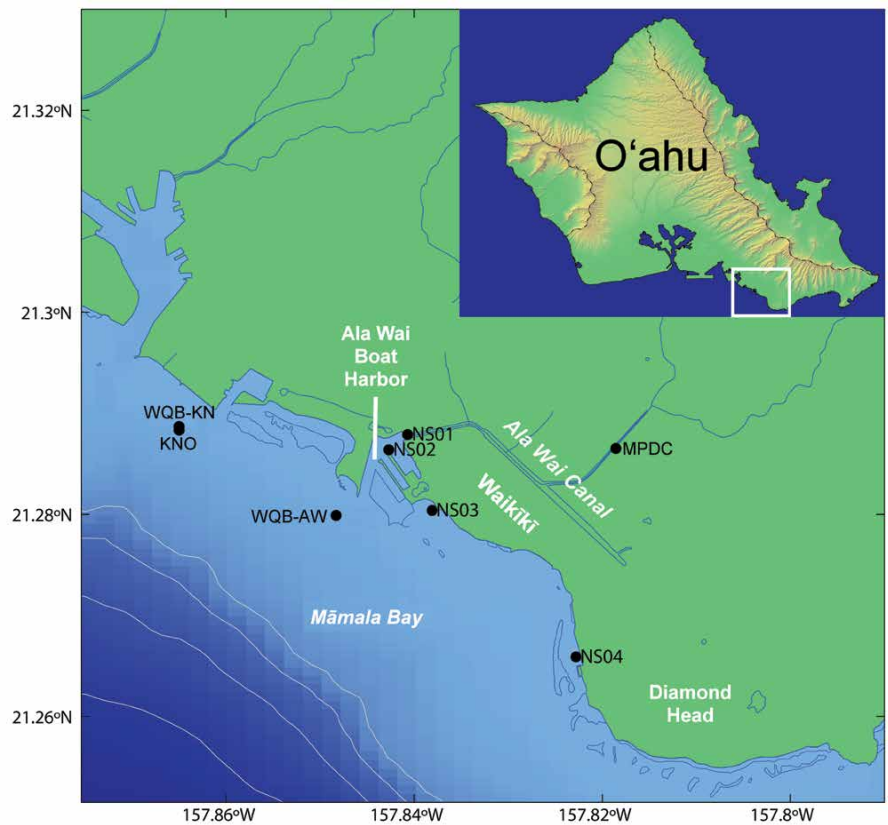


Figure 1. Overview of study area located on the south shore of O'ahu, Hawai'i, showing the Ala Wai Boat Harbor, Ala Wai Canal, and Māmala Bay. The figure also shows Pacific Islands Ocean Observing System (PacIOOS) nearshore sensors (NS01–04), water quality buoys (WQB-KN and WQB-AW), the Kilo Nalu cabled seafloor observatory (KNO), and the US Geological Survey's Mānoa-Pālolo Drainage Canal (MPDC) stream gauge.

and kept cool until filtered in the laboratory (within four hours). Samples were filtered through 0.22 μm capsule filters (Sterivex[®], Millipore) using a peristaltic pump. The filters were stored frozen (-80°C) until extracted. DNA was extracted from microorganisms collected on the filters as described previously (Nigro, 2012), using a modified version of the MasterPure[®] Kit (Epicentre) and passage through a column packed with polyvinylpyrrolidone to remove inhibitors.

Abundances of two pathogenic *Vibrio* were determined as genome-equivalent copy numbers by quantitative polymerase chain reaction (qPCR) assays of the purified DNA. The assays followed previously described protocols for *Vibrio parahaemolyticus* targeting the thermolabile hemolysin (*tlh*) gene (Nordstrom et al., 2007) and for *Vibrio vulnificus* targeting the *V. vulnificus* hemolysin (*VvhA*) gene (Campbell and Wright, 2003). All qPCR reactions were performed in triplicate with the

final replicate diluted tenfold to check for inhibition exactly as described for previous samples from the Ala Wai Canal (Nigro, 2012).

Differences among the abundance estimates for *V. parahaemolyticus* or *V. vulnificus* were tested for statistical significance using the SPSS[®] statistics software package (PASW Statistics v. 18.0; IBM Software). Mean abundances of duplicate samples were compared using a one-way ANOVA. Tukey's and Gabriel's post hoc tests were performed with the significance level set at $\alpha = 0.05$.

RESULTS

Water Level, Winds, and Waves

The first significant departure in the observed water level associated with the Chile tsunami was detected in the low-pass filtered pressure at the KNO ADCP at about 1145 HST on February 27, 2010 (Figure 2f). Water level observations at the NOS Honolulu tide gauge (#1612340, not shown) were very similar in amplitude and phase to the variations measured by the KNO ADCP. Measurable water level changes from the tsunami lasted for about four days. In order to separate the water level effects associated with the tsunami from water level effects associated with other phenomena, wind and wave data were also examined. Wind velocity measured at the NOS Honolulu tide gauge at the time of tsunami arrival was 4 m s^{-1} from the southwest, having shifted from variable winds three hours prior (Figure 2a). The change in wind velocity lasted for eight hours, from 0900–1700 HST. Variable winds prevailed from 1900 HST February 27 to 1500 HST February 28, and then returned to normal north-easterly tradewind conditions on February 28 (Figure 2a).

Background swell dominates the

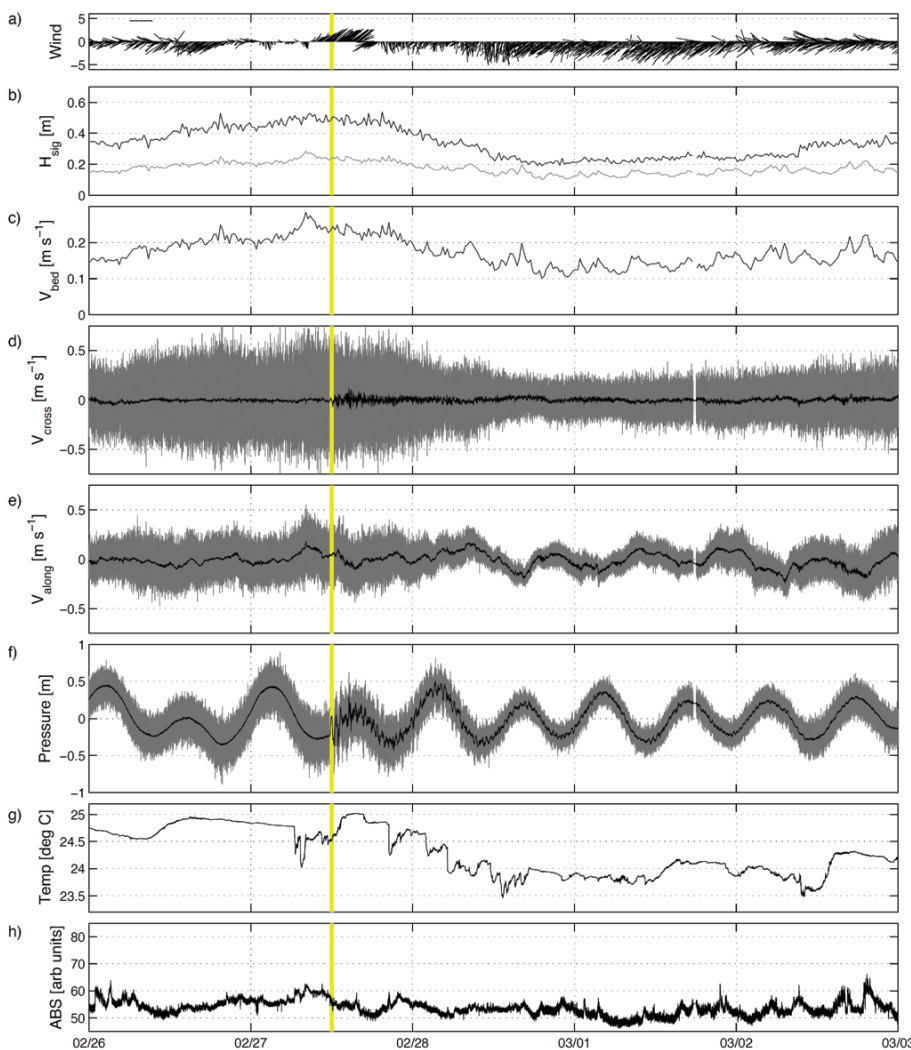


Figure 2. Data from the KNO during the 2010 Chile tsunami. (a) Wind vector data (from the NOS Honolulu tide gauge #1612340). (b) Significant wave height determined by the spectral method. (c) Near-bed current velocity. (d) Cross-shore depth-averaged currents. (e) Alongshore depth-averaged currents. (f) Pressure (expressed as meters). (g) Temperature at approximately 10 m depth. (h) Acoustic backscatter. The vertical yellow line indicates the first wave of the tsunami.

high-frequency pressure data at KNO (Figure 2f). Wave heights averaged every 20 minutes at KNO over several days before the 2010 Chile tsunami showed an increase in significant wave height to about 0.5 m, 36 hours prior to the wave arrival, followed by a decrease over the next 36 hours (Figure 2b) to about 0.2 m.

Near-bed velocity, calculated as the average of the highest one-third velocity measurements in the bottom 3 m over 20-minute intervals, primarily reflected wave-driven velocities, with no apparent response due to the tsunami (Figure 2c.) Low-pass filtered, depth-averaged velocities also remained relatively weak throughout the period (Figure 2d), with high frequencies reflecting wave flow and low-frequency flow responding to tides. Variations in the low-frequency velocity data showed a small increase (from $\sim 0.02 \text{ m s}^{-1}$ to 0.04 m s^{-1}) in alongshore velocity with the tsunami (Figure 2e). Variations in the corresponding cross-shore velocity component showed a sharp increase, with the highest velocities (0.1 m s^{-1}) occurring a few hours after the arrival of the first wave at 1445 HST (Figure 2d). Significant oscillations over the background levels persisted for the next 24 hours. Low-pass filtered pressure data also showed the highest amplitude variations a few hours after the initial wave arrival (Figure 2f).

The first significant departure in water level associated with the Japan tsunami occurred at KNO at 0320 HST on March 11, 2011 (Figure 3f). As for the Chile event, the NOS Honolulu tide gauge observations were very similar to those at KNO. Tsunami-produced water level changes were observed at both locations lasting about five days. Wind velocity at the time of the tsunami arrival was 1.3 m s^{-1} from the northeast, with winds increasing slightly throughout the

rest of the day.

Swell conditions for the Japan event (Figure 3b) were characterized by typical weak wintertime wave heights at roughly 0.3 m. Wave height values increased slightly with the arrival of the tsunami as the higher frequency tsunami components influenced the spectral wave height estimate. The tsunami arrival is more evident in the near-bed velocity (Figure 3c), reflecting contributions of the cross-shore velocities and somewhat weaker alongshore components

(Figure 3d,e) associated with the tsunami. The initial increase in water level is accompanied by an onshore velocity pulse with a weaker alongshore (southeast) component. The increase in low-passed velocity fluctuations is clearly notable for more than two days following the event. The strongest velocities ($> 0.2 \text{ m s}^{-1}$) occur later and persist over the next four hours, consistent with observations by Bricker et al. (2007) for the 2006 Kuril tsunami event, reflecting influence of local amplification.

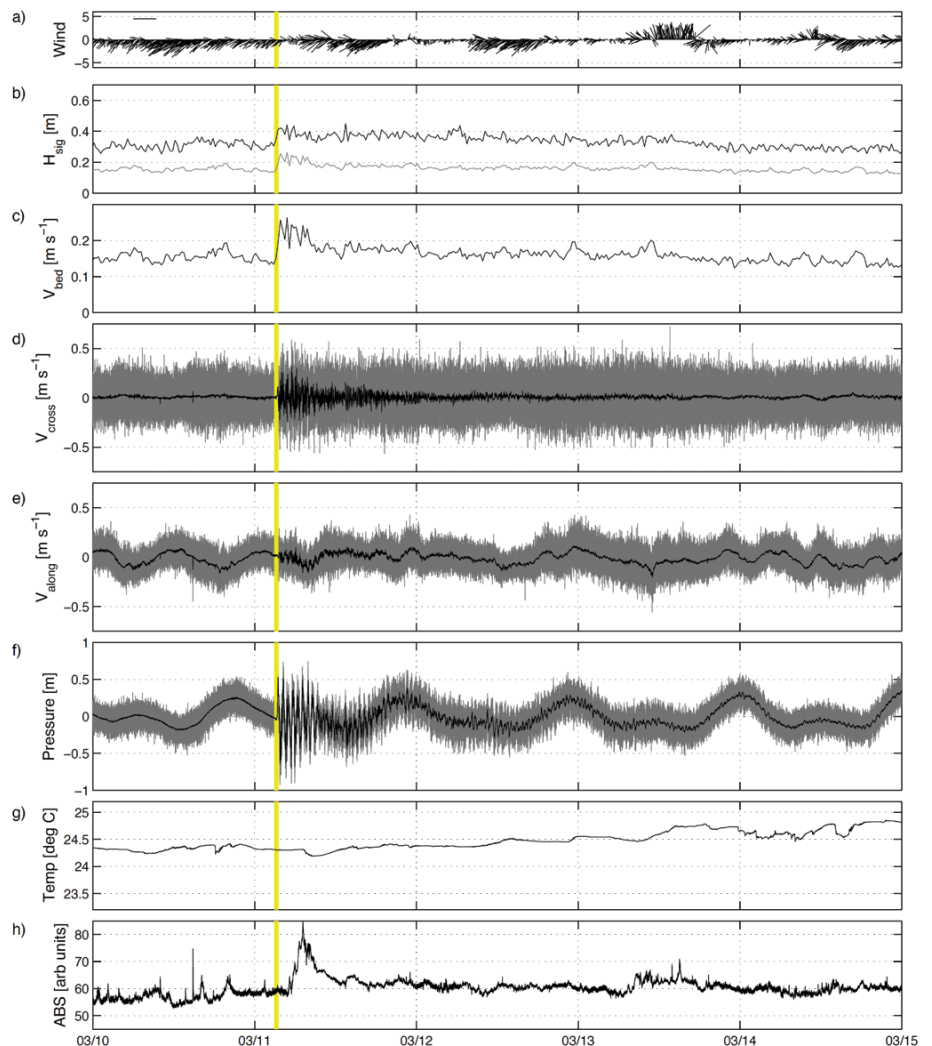


Figure 3. Data from the KNO during the 2011 Japan tsunami. (a) Wind vector data (from the NOS Honolulu tide gauge #1612340). (b) Significant wave height determined by the spectral method. (c) Near-bed current velocity. (d) Cross-shore depth-averaged currents. (e) Alongshore depth-averaged currents. (f) Pressure (expressed as meters). (g) Temperature at approximately 10 m depth. (h) Acoustic backscatter. The vertical yellow line indicates the first wave of the tsunami.

Spectral Energy

Spectral analysis of pressure data from the period of time following the two tsunamis revealed similar energy distributions, with the major spectral energy for both tsunamis occurring at approximately 43 minutes (Figure 4). Smaller energy peaks occurred on shorter time scales, between 12 and 18 minutes, or within 80–120 cpd. The greater energy resulting from the Japan tsunami yielded more coherent signal responses from all the sensors. During the Japan tsunami, the Ala Wai sensor, NS01, showed nearly twice the amount of energy at the 18-minute interval (80 cpd) than the coastal sensors NS03 and NS04 (Figure 4b). Spectral data at the KNO fore reef site showed a major peak near 43 minutes, along with a secondary peak at roughly 26 minutes (55 cpd). The KNO spectral data showed much lower

spectral energy than the nearshore sites at all frequencies for both events. A similar trend was apparent in analysis of the Japan tsunami by Yamazaki et al. (2012), where spectral amplitudes in Honolulu Harbor were larger relative to KNO. The observed spectral frequencies were consistent with previous analysis of the 2006 Kuril tsunami by Munger and Cheung (2008) that related periods of 16, 27, and 42 minutes to regional standing waves along the Hawaiian Islands. Bricker et al. (2007) related energy at periods of 3 to 8 minutes to smaller-scale edge waves trapped on the narrow island shelf. These waves account for significantly higher frequency peaks in the spectra for both events shown in Figure 4. High-frequency content at NS02 may also include contributions from seiche modes within the Ala Wai Canal excited by the tsunami arrivals.

Temperature

After an initial delay, the measured temperatures decreased at all sensors in the Ala Wai Canal and Māmalā Bay following the Chile tsunami (Figure 5b,c, respectively). NS01 and NS02 temperatures remained constant (at 25.5°C) for the first eight hours, then decreased by 2.5°C in the next 72 hours, and remained lower for 60 hours. NS03 and NS04 showed a larger decrease in temperature, both decreasing approximately 4°C over the 72 hours following the arrival of the first wave. The normal daily heating, calculated as the maximum temperature difference per day (0.65–1.91°C, over a two-month-long average centered around the tsunami) was reduced for all sensors except NS03 and NS04 for 24 hours following the tsunami, with the trend continuing at the WQBs for the next 48 hours. We elected to use the two month average temperature centered on initial tsunami arrival time to avoid factoring in any non-tsunami related short-period trends in temperature. Using this same approach, we observed that, in contrast, NS04, the farthest sensor from the mouth of Ala Wai Canal, showed increases in daily heating fluctuations for 72 hours after the tsunami. We also examined the water temperatures measured by WQB-AW three days prior to the arrival of the tsunami and three days after the arrival. The three-day average temperature decreased from 24.9°C to 24.3°C ($\Delta 0.6^\circ\text{C}$) after the arrival of the tsunami. At KNO, there were significant short time scale fluctuations in temperature over the tsunami time frame (Figure 2g). A longer time scale decrease in temperature was also evident in the days following the tsunami.

Interpretation of temperature data (and other variables) during the 2010 Chile tsunami was complicated by an

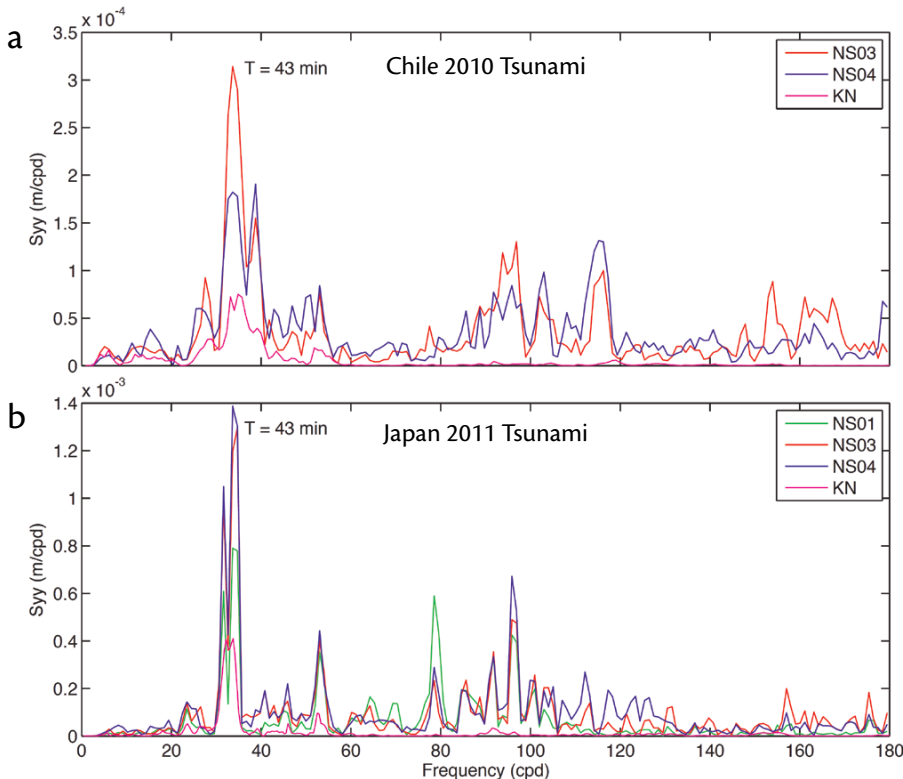


Figure 4. Spectral analysis of pressure variations at the nearshore sensors for three days following the first wave arrival of the (a) 2010 Chile, and (b) 2011 Japan tsunamis. Both tsunamis have peak energy at a period of approximately 43 minutes for all sensors.

increase in high-frequency fluctuations that began only hours before the arrival of the initial tsunami. These fluctuations are not uncommon at KNO and have been related to shoaling internal waves (Pawlak et al., 2009). This phenomenon will be addressed in greater detail in the discussion section below.

The long-term drop in temperature observed following the Chile tsunami did not occur following the Japan tsunami (Figure 6b,c), although slight deviations ($\Delta 0.3^{\circ}\text{C}$ at NS02) from the prevailing temperature trend occurred at all nearshore sensors with the arrival of the first wave. Daily heating variability was muted only at NS01 (-26%) when compared to a two-month-long average centered on the time of the tsunami. At NS04, as with the Chile tsunami, daily heating increased from the two-month-long average by $+20\%$. In contrast to the Chile tsunami, the three-day average temperature measured by WQB-AW increased slightly from 24.4°C to 24.6°C after the arrival of the tsunami.

Temperature at KNO for the Japan event (Figure 3g) shows a small decrease about four hours after the arrival of the first wave. This decrease might not be otherwise notable except that it coincides with a sharp increase in acoustic backscatter, discussed below.

Salinity

The Ala Wai Boat Harbor and Canal are tidally influenced. On flood tides, NS01 and NS02 routinely measure increased salinities as saline coastal waters enter the harbor and canal (Figure 5d). Conversely, during ebb tides, NS01 and NS02 measure decreased salinities—as freshwater is advected out of the harbor and canal. These salinity decreases are greater in magnitude during rain events, which can be estimated by non-tidally

influenced (typically asymmetrical) stage height increases in the hydrograph for MPDC, a tributary to the Ala Wai Canal. Thus, NS01 and NS02 naturally showed more variation in salinity measurements over the two months centered on the arrival of each tsunami, falling within ranges of $10.0\text{--}34.8$ ($\Delta 24.8$) at NS01, and $22.7\text{--}34.9$ ($\Delta 12.2$) at NS02, whereas

instruments farther from the canal (NS03, NS04, WQB-AW, and WQB-KN) exhibited a much smaller salinity range of $34.0\text{--}35.5$ ($\Delta 1.5$). Measured salinities in the Ala Wai Canal at NS01 and NS02 remained high (~ 33.5) and decreased in variability (remaining between 33.0 and 34.0) for 36 hours following an initial increase after the Chile tsunami

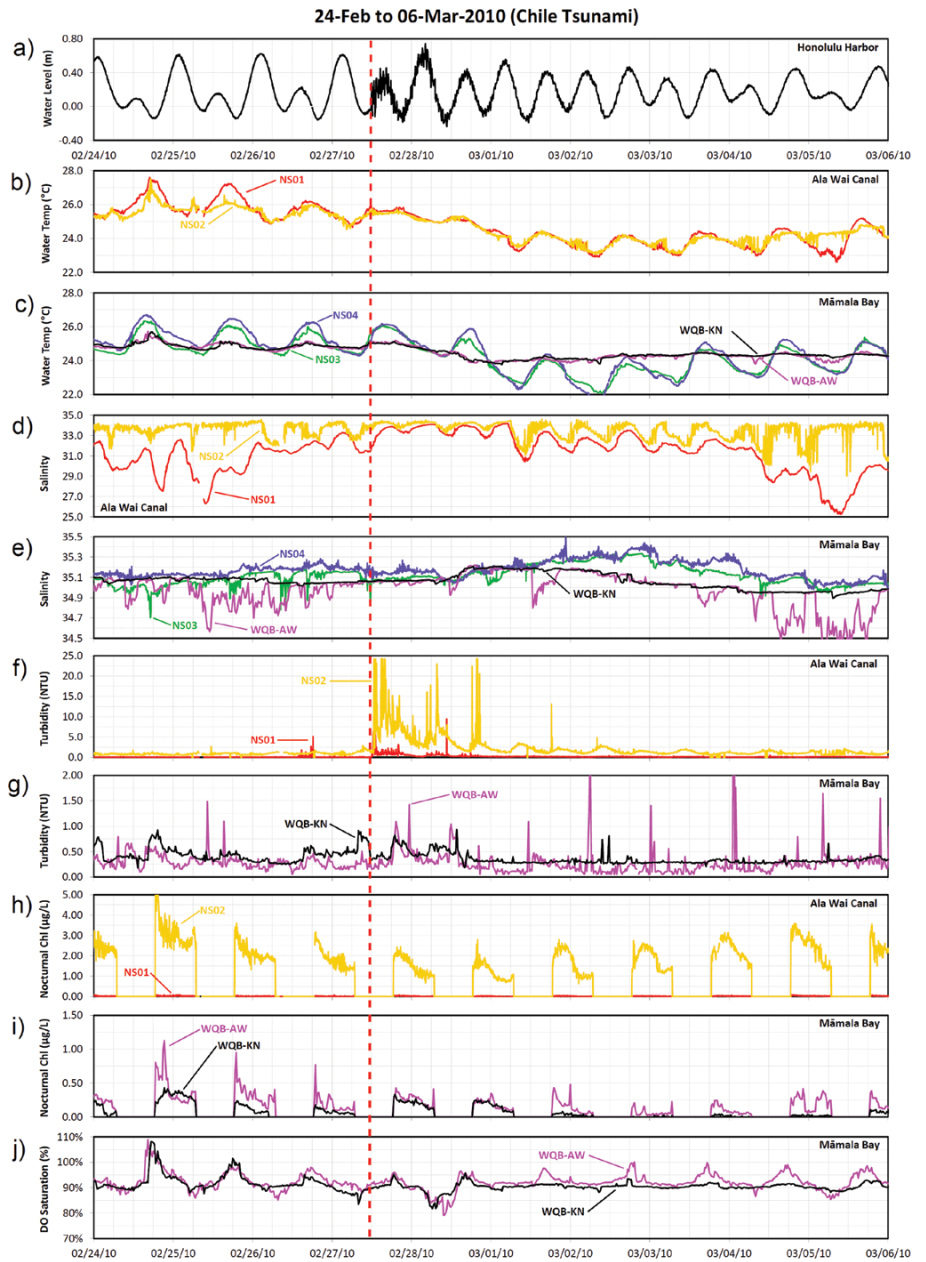


Figure 5. (a) Water level from the NOS Honolulu tide gauge. Ala Wai and Māmala Bay (b and c) water temperature, (d and e) salinity, (f and g) turbidity, and (h and i) chlorophyll, respectively. (j) Māmala Bay dissolved oxygen saturation data prior to and following the 2010 Chile tsunami.

(Figure 5d). Rainfall did not appear to have a discernible impact on NS01 and NS02 salinity measurements until five days after the tsunami on March 4, 2010. Instruments in Māmala Bay (NS03, NS04, WQB-KN and WQB-AW; Figure 5e) all showed smaller changes in salinity due to the tsunami relative to NS01 and NS02.

As in the Chile tsunami data, the salinity signal was also the most variable at NS01 before the Japan tsunami (Figure 6d). After the first wave (Figure 6a), both NS01 and NS02 exhibited a sharp drop (~ 2.0) in salinity, and both stabilized after three hours, between 33.0 and 34.0 (Figure 6d), then remained nearly constant until 22 hours after the

arrival of the first wave. Shortly after 0530 HST on March 12, high turbidity levels clogged the flow-through cell of the conductivity-temperature-depth (CTD) sensor of NS01. The sensor was cleaned at 1200 HST March 16, and data streams were restored. Following 0100 HST on March 12, NS02 showed increased variability, ranging from 34.0 to 29.0 within a six hour span on March 14. Unfortunately, due to the force of the Japan tsunami in the Ala Wai Boat Harbor, the Hawai'i Yacht Club pier hosting this sensor package was damaged. In order to avoid instrument loss, NS02 was retrieved from the pier just after 1200 HST on March 14, 2011. Except for a minor amount of rain (about 5 mm) in the upper reaches of the Ala Wai Canal watershed coincident with the arrival of the first tsunami wave, there was no measurable rainfall for the five days following the tsunami's arrival. Therefore, most of the salinity variation observed can be attributed to the effects of the tsunami.

Turbidity

Turbidity increased immediately following the arrival of the first wave of the Chile tsunami (Figure 5a), particularly at NS02 (Figure 5f). Prior to the arrival of the first wave, turbidity at NS02 was around 1.0 NTU; after the first wave, turbidity values of > 25 NTU (the maximum range of the sensor) occurred for three to four hours (Figure 5f). Turbidity values remained elevated at NS02 for at least three days after the tsunami. Turbidity also increased at NS01, but it rarely exceeded 5 NTU (Figure 5f). Offshore, turbidity measured by the WQBs was slightly elevated (Figure 5g).

The effects of the Japan tsunami on turbidity were more profound than the effects of the Chile tsunami. Following

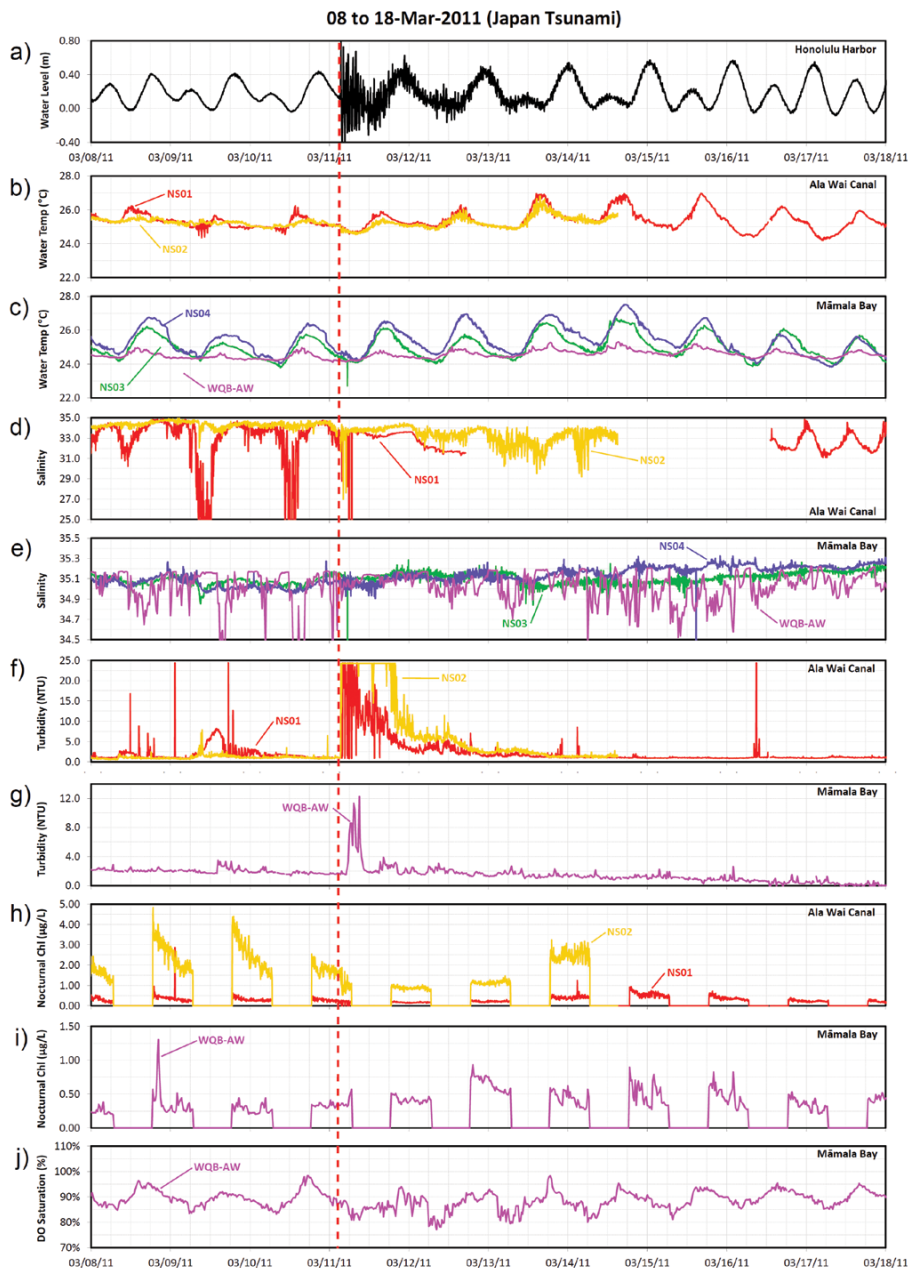


Figure 6. (a) Water level data from the NOS Honolulu tide gauge. Ala Wai and Māmala Bay (b and c) water temperature, (d and e) salinity, (f and g) turbidity, and (h and i) chlorophyll data, respectively. (j) Māmala Bay dissolved oxygen saturation data prior to and following the 2011 Japan tsunami.

the arrival of the first wave of the Japan tsunami (Figure 6a), turbidity increased rapidly in the Ala Wai Canal at NS01 and NS02 (Figure 6f) and in Māmalā Bay at WQB-AW (Figure 6g). At NS02, turbidity increased from ~ 1 NTU to > 25 NTU, exceeding the maximum range of the sensor, and remained > 25 NTU for 15 hours following the first wave (Figure 6f). Turbidity at NS01 also exceeded the maximum range of the sensor, after a delay of 40 minutes (10 samples), which was very close to the period of peak energy for both tsunamis. Unlike NS02, turbidity at NS01 did not remain at the maximum level for an extended period but instead was highly variable for ~ 3.5 hours following the first wave (Figure 6f). Turbidity at WQB-AW also began to increase from an initial measurement of 1.5 NTU after a delay of 100 minutes (five samples). The highest turbidity reading (12 NTU) occurred more than ~ 5.5 hours after the first wave, with turbidity returning to ~ 2 NTU some 7.5 hours after the first wave (Figure 6g). The time difference between the peak turbidity at the NS sensors and WQB-AW suggested the turbidity measured at WQB-AW was the result of the turbid plume issuing from the Ala Wai Canal. If the turbidity had been the result of bottom sediment resuspension in the vicinity of WQB-AW, in all likelihood, the peak would have occurred at very nearly the same time (and possibly earlier) than the peak observed at the NS locations.

Photographs taken of the Ala Wai Canal during the 2010 Chile tsunami showed resuspended sediment, most notably along the sides of the canal (Figure 7a). Because the 2011 Japan tsunami arrived in Hawai‘i during the dark early morning hours, photographic evidence of initial sediment resuspension

was unavailable. A photograph taken about 5.5 hours after the arrival of the first wave of the Japan tsunami showed more complete mixing of the Ala Wai Canal (Figure 7c) and, perhaps more importantly, a suspended sediment plume issuing from the mouth of MPDC and entering the Ala Wai Canal. Additionally, a photograph taken 10–12 hours after the arrival of the first wave showed a suspended sediment plume emanating from the Ala Wai Boat Harbor (see opening photo on title page) and entering Māmalā Bay.

Changes in turbidity on the fore reef at KNO could be inferred from the variations in acoustic backscatter (ABS) measured by the bottom-mounted ADCP. ABS was calculated from ADCP echo intensity data following Deines (1999), using generic coefficients for a 1,200 kHz ADCP. ABS values are uncalibrated so that units are in dB relative to an

arbitrary reference, but, in general, higher values represent an increase in suspended particulates at scales comparable to the acoustic wavelength, in this case roughly 1 mm. “Depth-averaged” ABS, shown in Figures 2h and 3h for the Chile and Japan events, respectively, excluded the upper 3 m to avoid surface and wave effects.

For the Chile tsunami, there was no detectable signal in ABS at KNO (Figure 2h). The depth-averaged data for the Japan event (Figure 3h), however, indicated a sharp increase at KNO roughly four hours after tsunami arrival.

Chlorophyll-*a*

Although the nearshore sensors (NS) and water quality buoys (WQB) collect measurements every four and every 20 minutes, respectively, we will only consider fluorescence measurements taken from sunset to sunrise. By



Figure 7. (a) Facing northwest along the Ala Wai Canal toward the mouth of the Mānoa-Pālolo Drainage Canal at 1208 HST on February 27, 2010, approximately eight minutes after the arrival of the first wave of the Chile tsunami at the Honolulu tide gauge. Note the sediment resuspension particularly along the sides of the canal. (b) Close-up photo of the mouth of the Mānoa-Pālolo Drainage Canal (MPDC) showing sediment entering the Ala Wai Canal from MPDC. (c) The Ala Wai Canal and Mānoa-Pālolo Drainage Canal at 0906 HST on March 11, 2011, approximately six hours after the first wave arrival of the Japan tsunami at the Honolulu tide gauge. Note that the tsunami-induced sediment plume is still issuing from the MPDC. *Photo credits: Ross Timmerman*

using only nighttime data, we avoid non-photochemical quenching of fluorescence (Figures 5h,i and 6h,i).

Following the 2010 Chile tsunami, chlorophyll (measured as fluorescence) at NS02 appeared to track the tides, with increasing chlorophyll at ebb tide and decreasing chlorophyll at flood tide (Figure 5h). Adjusting for a 56-minute lag behind the tidal signal, we found this pattern and the tidal signal to be moderately negatively correlated ($r = -0.613$) for the five nights following the tsunami. Other sensors did not show this effect.

Averages of nightly chlorophyll at NS02 decreased following both tsunamis. This trend was more pronounced with the 2011 Japan tsunami (Figure 6h), where average chlorophyll at NS02 decreased from $1.8 \mu\text{g L}^{-1}$ prior to the first wave to $1.0 \mu\text{g L}^{-1}$ after it. Prior to the tsunami, there was a regular nightly pattern of decreasing chlorophyll from the beginning to the end of the night. This pattern was absent for two nights after the Japan tsunami, and there was

reduced variability between samples, and significantly reduced fluorescence signals. On the third night after the tsunami, chlorophyll increased to an average of $2.5 \mu\text{g L}^{-1}$ and exhibited a larger variability between samples.

Pathogenic *Vibrios*

Shortly after the arrival of the Japan tsunami, the concentrations of *V. parahaemolyticus* and *V. vulnificus*, as determined by species-specific gene copy numbers, were 16.9 and 0.9 mL^{-1} . The concentrations of both species increased significantly late the following day by 200-fold ($p = 0.005$) and fivefold ($p = 0.002$), respectively, by which time turbidity had dropped to near baseline (Figure 8). By five days after the tsunami, concentrations of both species had declined significantly, twofold ($p = 0.014$) and fourfold ($p = 0.009$), respectively. At this point, abundances of both species were very similar to the geometric means calculated for 10 samples collected in 2008 and 2009 in the lower canal that

had similar temperature ($25\text{--}27^\circ\text{C}$) and salinity (31–34). None of the abundances following the tsunami were significantly different from the mean of those earlier samples (ANOVA, $p > 0.05$).

DISCUSSION

The turbidity data (Figures 5f,g and 6f,g) and the photographs of the Ala Wai Canal and Māmala Bay taken after the Chile and Japan tsunamis (Figure 7 and opening-spread photo) showed resuspension of the sediments in the Ala Wai Canal and MPDC as a result of the tsunamis. Although the Chile and Japan tsunamis were less than 1 m high by the time they arrived in Māmala Bay, they influenced turbidity from > 1 km inshore to at least 0.5 km offshore. Although suspended sediment plumes resulting from stormwater runoff are not unusual, the pattern exhibited by the plumes in the photographs, particularly after the Chile tsunami (Figure 7), differed from typical stormwater-related plumes and appeared to be controlled by water depth as evidenced by the prominence of the plume in shallower waters along the edges of the Ala Wai Canal. This pattern would not exist for a stormwater-derived suspended sediment plume where sediment load would be most likely associated with stream inputs (Tomlinson et al., 2011).

In an effort to provide perspective on the effects of the tsunamis on turbidity, we compared the turbidity data from NS02 and WQB-AW during the 2011 Japan tsunami to that from a 24-hour rainstorm with a recurrence interval of one year (i.e., the one-year, 24-hour storm) that occurred during March 2009 (Figure 9). The horizontal axis (time) was converted from actual time to elapsed time, where time zero was the onset of rainfall during the March 2009

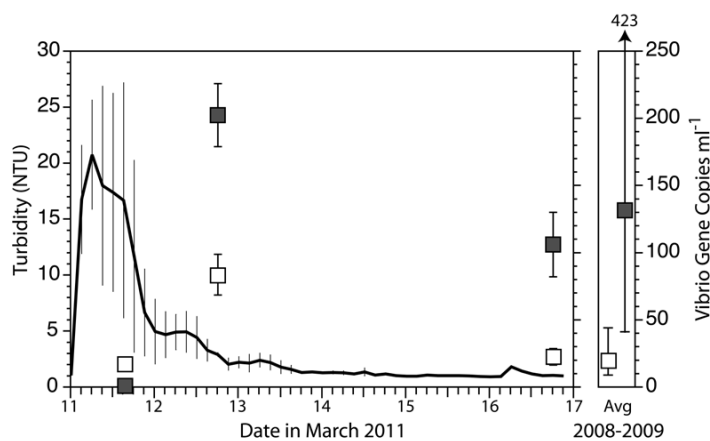


Figure 8. Turbidity (solid line) and the concentrations of *Vibrio parahaemolyticus* (shaded squares) and *V. vulnificus* (open squares) determined from gene copy numbers of *tlh* and *VvhA* genes, respectively. Turbidity is shown as the tri-hourly averaged mean (\pm s.d.) for NS01 and NS02, up until March 14, after which only NS01 data were available. Gene copy numbers in the left panel are shown as the mean (\pm s.d.) for duplicate qPCR assays. Gene copy numbers in the right panel are the geometric means (\pm s.d.) for samples collected in the lower Ala Wai Canal between 2008 and 2009 ($n = 10$). Only samples having a temperature between 25°C and 27°C and a salinity of 31–36 were used for the comparison.

storm and the arrival of the first wave during the March 2011 tsunami. Figure 9 shows that the turbidity effects of the Japan tsunami were comparable to the effects of the one-year, 24-hour rainstorm, except for the timing of the onset. Elevated turbidity values occurred immediately upon the arrival of the first tsunami wave, whereas the storm-related turbidity increased about six hours after the onset of the rain.

The sediments that accumulate in the Ala Wai Canal and MPDC are sinks for various pollutants associated with stormwater runoff and, to a lesser degree, from the atmosphere, along with pollutants from the Ala Wai Boat Harbor. When these sediments are resuspended, changes in environmental conditions (e.g., temperature, salinity, pH, oxidation-reduction potential) can affect the partitioning of the pollutants between the water and the suspended sediment (Stumm and Morgan, 1996). Regardless of whether these pollutants are dissolved in the water column or associated with the suspended sediments, the pollutant load to the coastal ocean can increase during even a small tsunami, if only for a brief time, as a result of sediment resuspension.

Although considerable data were available on pollutants in the Ala Wai Canal and Boat Harbor sediments prior to 2003 dredging there (De Carlo and Spencer, 1995; De Carlo and Anthony, 2002; De Carlo et al., 2004), no published data are available on the pollutants in the sediments following the dredging. However, considerable data are available on pollutants in suspended particles in the streams that empty into the Ala Wai Canal, particularly Mānoa Stream. De Carlo et al. (2005) reported elevated concentrations of Cr, Cu, Ni, Zn, Pb, Cd, and As in Mānoa Stream at

Kānewai Park 1.9 km upstream of the Ala Wai Canal. The first three elements (Cr, Cu, and Ni) are primarily petrogenic in origin; the remaining elements are considered to have primarily anthropogenic sources. In addition to these trace elements, according to Anthony et al. (2004), various organochlorine termiticides such as dieldrin and chlordane, even though discontinued in the 1980s (Takahashi, 1982), persist in the soils of Mānoa Valley, and hence, in Mānoa Stream sediments as a result of erosion during storms. These persistent, hydrophobic organochlorine compounds bind strongly to soils (Neilson, 1994) and are carried as sediments downstream, presumably as far as the Ala Wai Canal. Anthony et al. (2004) also report the presence of PCBs, DDT compounds, polyaromatic hydrocarbons, and phthalates, in Mānoa Stream sediments. The pollutants in the sediments of Mānoa Stream (and other streams) are carried to the Ala Wai Canal and Boat Harbor. According to the Hawai'i State Department of Health (2008), pollutants

found in the Ala Wai Canal and Boat Harbor include nutrients, pathogens, suspended solids, organochlorine pesticides, and lead and other metals. Many of these pollutants reside in the sediments and are released to the coastal ocean upon resuspension.

Another health concern with respect to the waters of the Ala Wai Canal and Harbor is the presence of pathogenic *Vibrio* bacteria, such as *V. parahaemolyticus* and *V. vulnificus*. The latter species was implicated in the death of an individual exposed to harbor waters in 2006 (Creamer and Moreno, 2006; Venzon, 2007). Because pathogenic *Vibrio* are indigenous to the estuarine waters of the canal, they display different dynamics from sediment-derived pollutants. The data presented here suggest that *Vibrio* abundances changed significantly in the days following the tsunami, but we cannot be certain that these changes were a direct effect of the tsunami. Shortly after the tsunami arrived and when turbidity was still high, *Vibrio* abundances were low, most

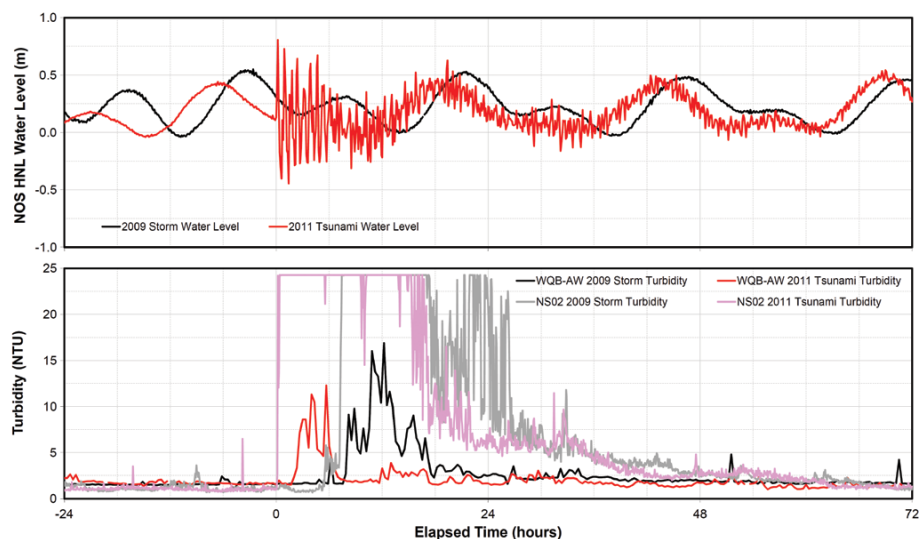


Figure 9. Water level measured at the Honolulu tide gauge (top panel) and turbidity (bottom panel) at NS02 (Ala Wai Canal) and WQB-AW (Māmala Bay) during the March 2009 one-year, 24-hour storm and the March 2011 Japan tsunami. Note that, other than timing, the magnitude of the turbidity effects of the storm and tsunami are very similar.

likely because of dilution by mixing. The significant rise in both *Vibrio* species on the following day could have been a result of advection, but may also reflect stimulation of *Vibrio* growth on dissolved organic matter resuspended from the sediments. The subsequent decline in *Vibrio* concentrations to average values when next measured five days

residence time of water within the lower harbor. This increased mixing in the nearshore waters would also potentially lead to cross-shore amplification of chemical and biological signals that are evident in sensor data. Increased mixing may also have led to the initial two-day decrease and subsequent increase in nightly chlorophyll levels seen after the

back reef lagoon located between Kewalo Basin and the Ala Wai Canal.

Like Laluraj et al. (2007), we also observed a general decrease in water temperature during the Chile tsunami (Figure 5b,c) but, interestingly, not during the more powerful Japan tsunami. As mentioned earlier, there may have been a confounding factor during the 2010 Chile tsunami. Time-series plots of WQB-AW data for about three days before and seven days after the arrival of the tsunamis reveal a phenomenon that is particularly evident in the salinity plot for the Chile tsunami (Figure 5e). A close examination of these data indicates that salinity was almost exclusively oceanic for about six hours before the tsunami arrived, and this condition, with some variation, persisted for five days. We examined the 2010 and 2011 annual plots and noted that similar events or “oceanic episodes,” typically lasting two to five days, had occurred four to five times from about January through April, and thus could not be deemed to be derived exclusively from the tsunamis. In 2010, however, there was no pronounced decrease in water temperature during these oceanic episodes, except following the Chile tsunami, suggesting that the tsunami may have affected water temperature.

A comparison of the data from the two tsunamis shows several other interesting effects. The effects on nearshore turbidity have already been discussed, but it is notable that the increase in turbidity during the Japan tsunami was considerably greater than during the Chile tsunami. While all other variable scales were equal for the two tsunamis, the 2011 turbidity scale for Māmalā Bay (Figure 6g) is seven times the 2010 turbidity scale (Figure 5g). The elevated turbidity values in the

“ THE CHILE AND JAPAN TSUNAMIS, OCCURRING ROUGHLY A YEAR APART, PROVIDED A UNIQUE OPPORTUNITY TO COMPARE THEIR EFFECTS IN MĀMALĀ BAY, O’AHU, HAWAII, AND IN ITS TRIBUTARIES UNDER SIMILAR WEATHER CONDITIONS. ”

after the tsunami suggests that any effect of the tsunami on *Vibrio* abundance was relatively short lived. The range of pathogenic *Vibrio* concentrations in the days following the tsunami spanned a range similar to that recorded during a previous year-long study of the canal (Nigro, 2012). These data suggest that, if the tsunami was responsible for changes in the abundance of *Vibrio*, its effect was similar in magnitude to changes driven by other environmental drivers such as runoff from rainfall.

Following both the Chile and Japan tsunamis, the lower Ala Wai Boat Harbor became completely mixed. The similarity of salinity and turbidity values at NS01 and NS02 after both tsunamis suggests that water within the harbor became close to homogenous; the higher flushing rates from the tsunami contributed to the influx of colder and more saline offshore water, as well as a shorter

2011 Japan tsunami. Reduced clarity in the water from sediment resuspension would decrease light availability, while also potentially increasing nutrient load (e.g., De Carlo et al., 2007; Tomlinson et al., 2011).

The increases in acoustic backscatter observed at KNO for the Japan event suggested that suspended solids from nearshore sites did, in fact, affect coastal fore reef environments. The delay in acoustic backscatter increase relative to the tsunami arrival (Figures 2h, 3h) indicated that the tsunami did not result in any significant sediment suspension at the KNO site. Average alongshore velocities were to the west following the event, increasing to about 0.1 m s^{-1} toward the northwest (toward KNO and away from Waikiki), suggesting a source for the acoustic backscatter increase within about 1 km, consistent with Kewalo Basin Boat Harbor or the Ala Moana

Ala Wai estuary and coastal ocean that lasted for several days after the arrival of both tsunamis generally agrees with the decrease in Secchi depth reported by Laluraj et al. (2007).

Only the WQBs were equipped with dissolved oxygen (DO) sensors. While we did not see the “drastic” reduction in DO reported by Reddy et al. (2005), the DO saturation minima were depressed by about 5% following the Chile and Japan tsunamis, and the diel cycle in DO was considerably dampened during the Chile tsunami.

WQB-AW was not equipped with a Satlantic ISUS V3[®] nitrate sensor until late in 2010; therefore, we cannot comment on nitrate concentrations during the Chile tsunami. Unlike Reddy et al. (2005) and Laluraj et al. (2007), we did not see an increase in nitrate following the Japan tsunami. In fact, we observed a slight decrease following this tsunami. There was, however, an increase in chlorophyll for about five days following the Japan tsunami. Given that the turbidity was never very high offshore and decreased rapidly to values < 4 NTU following the tsunami, it is possible a small phytoplankton bloom occurred, causing increased chlorophyll and decreased nitrate concentrations. Conversely, Sarangi (2011) noted an increase in chlorophyll in the Bay of Bengal following the 2004 Indian Ocean tsunami and in the Pacific Ocean (presumably) following the 2011 Japan tsunami.

It is important to note that the tsunami warning for Hawai'i following the 2011 earthquake off Japan was canceled at 1200 HST on March 11, 2011, less than nine hours after the arrival of the first wave. Given that elevated turbidity values (i.e., > 5 NTU) were measured in the Ala Wai Canal for 36 hours after the first wave, and that levels of pathogenic

microorganisms were elevated 24 hours after the first wave, the water quality effects lasted significantly longer than the warnings. Public awareness of tsunami safety is generally limited to water levels and waves, and many beach-goers return to the waters of Waikiki not long after the warning cancellations. Data from the PacIOOS sensors and our sampling show that altered and potentially degraded water quality conditions can persist longer than the physical threat from surge. Hence, there should be expanded and continued monitoring following such events in order to accurately characterize their impact on water quality and evaluate potential public health risks.

PacIOOS data show that relatively small tsunamis can profoundly affect water quality, most notably turbidity, in estuarine areas and the coastal ocean. These effects can be equivalent to storms, with a statistical recurrence interval on the order of one year. Moreover, the effects can extend offshore at least 0.5 km and last for several days. It is important that human health agencies account for these water quality effects when issuing an “all clear.” While the danger associated with high waves and strong currents may have dissipated, water quality effects can linger for several days and may affect a relatively large area.

ACKNOWLEDGEMENTS

We would like to thank two anonymous reviewers and *Oceanography* Editor Ellen Kappel for their careful review of our draft manuscript. Their thoughtful comments and suggestions greatly improved the final document and the data products contained herein. We would also like to acknowledge the support of NOAA through Cooperative Agreements NA10NOS47300167 and

NA11NOS0120039 and additional funding for bacterial analyses from Sea Grant (NOAA Grant NA09OAR4170060), as well as the many support personnel who made this study possible. They include Jeff Sevadjan (study area graphics), Sarah Feinman (nearshore technician), Gordon Walker (nearshore technician), and Conor Jerolmon (nearshore technician). 

REFERENCES

- Anthony, S.S., C.D. Hunt Jr., A.M.D. Brasher, L.D. Miller, and M.S. Tomlinson. 2004. *Water Quality on the Island of Oahu, Hawaii: 1999–2001*. USGS Circular 1239. US Geological Survey, Reston, VA, 37 pp, <http://pubs.usgs.gov/circ/2004/1239/pdf/circular1239.pdf> (accessed February 3, 2014).
- Bricker, J.D., S. Munger, C. Pequignet, J.R. Wells, G. Pawlak, and K.F. Cheung. 2007. ADCP observations of edge waves off Oahu in the wake of the November 2006 Kuril Islands tsunami. *Geophysical Research Letters* 34, L23617, <http://dx.doi.org/10.1029/2007GL032015>.
- Campbell, M.S., and A.C. Wright. 2003. Real-time PCR analysis of *Vibrio vulnificus* from oysters. *Applied Environmental Microbiology* 69:7,137–7,144, <http://dx.doi.org/10.1128/AEM.69.12.7137-7144.2003>.
- Chandrasekharan, H., A. Sarangi, M. Nagarajan, V.P. Singh, D.U.M. Rao, P. Stalin, K. Natarajan, B. Chandrasekaran, and S. Anbazhagan. 2008. Variability of soil–water quality due to Tsunami-2004 in the coastal belt of Nagapattinam district, Tamilnadu. *Journal of Environmental Management* 89:63–72, <http://dx.doi.org/10.1016/j.jenvman.2007.01.051>.
- Cremer, B., and L. Moreno. 2006. ‘Horrible, horrible death’ by infection. *Honolulu Advertiser* April 8, 2006. Gannett Company Inc., Honolulu, <http://the.honoluluadvertiser.com/article/2006/Apr/08/In/FP604080336.html> (accessed February 3, 2014).
- De Carlo, E.H., and S.A. Anthony. 2002. Spatial and temporal variability of trace element concentrations in an urban subtropical watershed, Honolulu, Hawaii. *Applied Geochemistry* 17:475–492, [http://dx.doi.org/10.1016/S0883-2927\(01\)00114-7](http://dx.doi.org/10.1016/S0883-2927(01)00114-7).
- De Carlo, E.H., V.L. Beltran, and M.S. Tomlinson. 2004. Composition of water and suspended sediment in streams of urbanized subtropical watersheds in Hawaii. *Applied Geochemistry* 19:1,011–1,037, <http://dx.doi.org/10.1016/j.apgeochem.2004.01.004>.
- De Carlo, E.H., D.J. Hoover, C.W. Young, R.S. Hoover, and F.T. Mackenzie. 2007. Impact of storm runoff from subtropical watersheds on

- coastal water quality and productivity. *Applied Geochemistry* 22:1,777–1,797, <http://dx.doi.org/10.1016/j.apgeochem.2007.03.034>.
- De Carlo, E.H., and K.J. Spencer. 1995. Records of lead and other heavy metal inputs to sediments of the Ala Wai Canal, Oahu, Hawaii. *Pacific Science* 49(4):471–491.
- De Carlo, E.H., M.S. Tomlinson, and S.S. Anthony. 2005. Trace elements in streambed sediments of small subtropical streams on O'ahu, Hawai'i: Results from the USGS NAWQA program. *Applied Geochemistry* 20:2,157–2,188, <http://dx.doi.org/10.1016/j.apgeochem.2005.08.005>.
- Deines, K.L. 1999. Backscatter estimation using broadband acoustic Doppler current profilers. Pp. 249–253 in *Proceedings IEEE Sixth Working Conference on Current Measurement*, San Diego, CA, March 11–13, 1999, <http://dx.doi.org/10.1109/CCM.1999.755249>.
- Dharanirajan, K., P. Kasinatha Pandian, B. Gurugnanam, R.M. Narayanan, and S. Ramachandran. 2007. An integrated study for the assessment of tsunami impacts: A case study of South Andaman Island, India using remote sensing and GIS. *Coastal Engineering Journal* 49:229–266, <http://dx.doi.org/10.1142/S0578563407001617>.
- Elango, L., A. Das, S. Chidambaram, S. Kaliappan, J.F. Lawrence, K. Palanivel, and R. Ravichandran. 2006. Water quality in the coastal areas of Tamilnadu after tsunami. Pp. 45–58 in *26th December 2004 Tsunami: Causes, Effects, Remedial Measures, Pre- and Post-Tsunami Disaster Management. A Geoscientific Perspective*. G.V. Rajamanickam, B.R. Subramanian, M. Baba, R. Ramesh, L. Elango, and M. Prithviraj, eds, Earth System Science, Department of Science and Technology, Government of India, New Delhi.
- Hawai'i State Department of Health. 2008. *2006 State of Hawaii Water Quality Monitoring and Assessment Report: Integrated Report to the US Environmental Protection Agency and the US Congress Pursuant to Sections §303(d) and §305(b), Clean Water Act (PL 97-117)*. Hawai'i State Department of Health, Honolulu, HI, 279 pp., http://health.hawaii.gov/cwb/files/2013/05/Integrated_2006_StateOfHawaii.pdf (accessed February 3, 2014).
- Laluraj, C.M., V. Kesavadas, K.K. Balachandran, V.J. Gerson, G.D. Martin, P. Shaiju, C. Revichandran, T. Joseph, and M. Nair. 2007. Recovery of an estuary in the southwest coast of India from tsunami impacts. *Environmental Monitoring and Assessment* 125:41–45, <http://dx.doi.org/10.1007/s10661-006-9237-2>.
- Mattsoson, E., M. Ostwald, S.P. Nissanka, B. Holmer, and M. Palm. 2009. Recovery and protection of coastal ecosystems after tsunami event and potential for participatory forestry CDM: Examples from Sri Lanka. *Ocean & Coastal Management* 52:1–9, <http://dx.doi.org/10.1016/j.ocecoaman.2008.09.007>.
- Mori, N., T. Takahashi, T. Yasuda, and H. Yanagisawa. 2011. Survey of 2011 Tohoku earthquake tsunami inundation and run-up. *Geophysical Research Letters* 38, L00G14, <http://dx.doi.org/10.1029/2011GL049210>.
- Munger, S., and K.F. Cheung. 2008. Resonance in Hawaii waters from the 2006 Kuril Islands tsunami. *Geophysical Research Letters* 35, L07605, <http://dx.doi.org/10.1029/2007GL032843>.
- National Geophysical Data Center. 2011a. March 11, 2011 Japan Earthquake and Tsunami. http://www.ngdc.noaa.gov/hazard/tsunami/pdf/2011_0311.pdf (accessed June 20, 2011).
- National Geophysical Data Center. 2011b. Historical Tsunami Database. http://www.ngdc.noaa.gov/hazard/tsu_db.shtml (accessed June 20, 2011).
- Neilson, A.H. 1994. *Organic Chemicals in the Aquatic Environment: Distribution, Persistence, and Toxicity*. CRC Press, Boca Raton, FL, 438 pp.
- Newton, A., and J. Icelly. 2008. Land ocean interactions in the coastal zone, LOICZ: Lessons from Banda Aceh, Atlantis, and Canute. *Estuarine, Coastal and Shelf Science* 77(2008):181–184, <http://dx.doi.org/10.1016/j.ecss.2007.09.016>.
- Nigro, O.D. 2012. Environmental controls on *Vibrio vulnificus* and other pathogenic *Vibrios* in tropical and subtropical coastal waters. PhD Dissertation, University of Hawai'i at Mānoa.
- Nordstrom, J.L., M.C.L. Vickery, G.M. Blackstone, S.L. Murray, and A. DePaola. 2007. Development of a multiplex real-time PCR assay with an internal amplification control for the detection of total and pathogenic *Vibrio parahaemolyticus* bacteria in oysters. *Applied Environmental Microbiology* 73:5,840–5,847, <http://dx.doi.org/10.1128/AEM.00460-07>.
- Pacific Tsunami Warning Center/National Oceanic and Atmospheric Administration/National Weather Service. 2010. Tsunami Bulletin Number 005, February 27, 2010. <http://www.prh.noaa.gov/ptwc/messages/pacific/2010/pacific.2010.02.27.104329.txt> (accessed June 20, 2011).
- Pawlak, G., E. De Carlo, J. Fram, A. Hebert, C. Jones, B. McLaughlin, M. McManus, K. Millikan, F. Sansone, T. Stanton, and J. Wells. 2009. Development, deployment, and operation of Kilo Nalu Nearshore Cabled Observatory. Paper presented at IEEE OCEANS 2009 Conference, Bremen.
- Reddy, H.R.V., R.J. Katti, K.P. Raveesha Chandrashekar, S.J. Vikas, R.S. Nagendra Babu, and K.S. Shiva Kumar. 2005. Coastal water quality off Dakshina Kannada before and after tsunami. Correspondence. *Current Science* 88(7):1,026–1,027.
- Sarang, R.K. 2011. Remote sensing of chlorophyll and sea surface temperature in Indian water with impact of 2004 Sumatra tsunami. *Marine Geodesy* 34:152–166, <http://dx.doi.org/10.1080/01490419.2011.571561>.
- Star-Advertiser Staff. March 11, 2011. 200 boats damaged; harbors remain closed after tsunami strikes. <http://www.staradvertiser.com/news/bulletin/117789823.html> (accessed June 20, 2011).
- Stumm, W., and J.J. Morgan. 1996. *Aquatic Chemistry: Chemical Equilibria and Rates in Natural Waters*, 3rd ed. John Wiley & Sons, Inc., New York, NY, 1,022 pp.
- Takahashi, W. 1982. *Pesticide Usage Patterns in Hawaii, 1977*. Pesticide Hazard Assessment Project, Pacific Biomedical Research Center, University of Hawai'i, Honolulu, HI, 92 pp.
- Tanabe, S., and A. Subramanian. 2011. Great eastern Japan earthquake: Possible marine environmental contamination by toxic pollutants. *Marine Pollution Bulletin* 62:883–884, <http://dx.doi.org/10.1016/j.marpolbul.2011.04.033>.
- Tomlinson, M., E.H. De Carlo, M. McManus, E. Pawlak, G. Steward, F. Sansone, O. Nigro, C. Ostrander, R. Timmerman, J. Patterson, and S.J. Uribe. 2011. Characterizing the effects of two storms on the coastal waters of O'ahu, Hawai'i, using data from the Pacific Islands Ocean Observing System. *Oceanography* 24(2):182–199, <http://dx.doi.org/10.5670/oceanog.2011.38>.
- Venzon, N.C. Jr. 2007. Massive discharge of untreated sewage into the Ala Wai Canal (Oahu, Hawaii): A threat to Waikiki's waters? *Journal of Environmental Health* 70(5):25–30.
- Violette, S., G. Boulicot, and S.M. Gorelick. 2009. Tsunami-induced groundwater salinization in southeastern India. *Comptes Rendus Geoscience* 341:339–346, <http://dx.doi.org/10.1016/j.crte.2008.11.013>.
- Yamazaki, Y., K.F. Cheung, G. Pawlak, and T. Lay. 2012. Surges along the Honolulu coast from the 2011 Tohoku tsunami. *Geophysical Research Letters* 39, L09604, <http://dx.doi.org/10.1029/2012GL051624>.